



**AFRL-RY-WP-TP-2011-1008**

**DYNAMIC BEHAVIOR OF AN INJECTION-LOCKED  
QUANTUM-DASH FABRY-PEROT LASER AT ZERO-  
DETUNING (POSTPRINT)**

**Mike Pochet, Nader A. Naderi, and Luke F. Lester**

**University of New Mexico**

**Nathan B. Perry and Vassilios Kovanis**

**Electro-optic Components Technology Branch  
Aerospace Components Division**

**JULY 2010**

**Approved for public release; distribution unlimited.**

*See additional restrictions described on inside pages*

**STINFO COPY**

**© 2009 Optical Society of America**

**AIR FORCE RESEARCH LABORATORY  
SENSORS DIRECTORATE  
WRIGHT-PATTERSON AIR FORCE BASE, OH 45433-7320  
AIR FORCE MATERIEL COMMAND  
UNITED STATES AIR FORCE**

REPORT DOCUMENTATION PAGE				Form Approved OMB No. 0704-0188	
The public reporting burden for this collection of information is estimated to average 1 hour per response, including the time for reviewing instructions, searching existing data sources, gathering and maintaining the data needed, and completing and reviewing the collection of information. Send comments regarding this burden estimate or any other aspect of this collection of information, including suggestions for reducing this burden, to Department of Defense, Washington Headquarters Services, Directorate for Information Operations and Reports (0704-0188), 1215 Jefferson Davis Highway, Suite 1204, Arlington, VA 22202-4302. Respondents should be aware that notwithstanding any other provision of law, no person shall be subject to any penalty for failing to comply with a collection of information if it does not display a currently valid OMB control number. PLEASE DO NOT RETURN YOUR FORM TO THE ABOVE ADDRESS.					
1. REPORT DATE (DD-MM-YY) July 2010		2. REPORT TYPE Journal Article Postprint		3. DATES COVERED (From - To) 15 September 2008 – 31 July 2010	
4. TITLE AND SUBTITLE DYNAMIC BEHAVIOR OF AN INJECTION-LOCKED QUANTUM-DASH FABRY-PEROT LASER AT ZERO-DETUNING (POSTPRINT)				5a. CONTRACT NUMBER	
				5b. GRANT NUMBER FA8750-06-1-0085	
				5c. PROGRAM ELEMENT NUMBER 62500F	
6. AUTHOR(S) Mike Pochet, Nader A. Naderi, and Luke F. Lester (University of New Mexico) Nathan B. Perry and Vassilios Kovanis (AFRL/RYPD)				5d. PROJECT NUMBER 5028	
				5e. TASK NUMBER RL	
				5f. WORK UNIT NUMBER 528DSN04	
7. PERFORMING ORGANIZATION NAME(S) AND ADDRESS(ES) University of New Mexico Center for High Technology Materials 1313 Goddard SE Albuquerque, NM 87106				8. PERFORMING ORGANIZATION REPORT NUMBER	
Electro-optic Components Technology Branch (AFRL/RYPD) Aerospace Components Division Air Force Research Laboratory, Sensors Directorate Wright-Patterson Air Force Base, OH 45433-7320 Air Force Materiel Command, United States Air Force					
9. SPONSORING/MONITORING AGENCY NAME(S) AND ADDRESS(ES) Air Force Research Laboratory Sensors Directorate Wright-Patterson Air Force Base, OH 45433-7320 Air Force Materiel Command United States Air Force				10. SPONSORING/MONITORING AGENCY ACRONYM(S) AFRL/RYPD, AFOSR	
				11. SPONSORING/MONITORING AGENCY REPORT NUMBER(S) AFRL-RY-WP-TP-2011-1008	
12. DISTRIBUTION/AVAILABILITY STATEMENT Approved for public release; distribution unlimited.					
13. SUPPLEMENTARY NOTES Journal article published in <i>Optics Express</i> , Vol. 17, No. 23, November 9, 2009. © 2009 Optical Society of America. The U.S. Government is joint author of the work and has the right to use, modify, reproduce, release, perform, display, or disclose the work. This work is one of a number of manuscripts published in peer-reviewed journals as a result of in-house work on technical report AFRL-RY-WP-TR-2010-1195. This paper contains color and is available to the public.					
14. ABSTRACT This work investigates the behavior of a zero-detuned optically-injected quantum-dash Fabry-Perot laser as the injected field ratio is increased from near-zero to levels resulting in stable locking. Using a normalized model describing optically-injected semiconductor lasers, variations in the slave laser's free-running characteristics are shown to have a strong impact on the coupled system's behavior. The theoretical model is verified experimentally using a high resolution spectrometer. It is found that the quantum-dash laser has the technological advantage of a low linewidth enhancement factor at low bias currents that suppresses undesirable Period-2 and chaotic behavior. Such observations suggest that optically-injected quantum-dash lasers can be used as an enabling component for tunable photonic oscillators.					
15. SUBJECT TERMS semiconductor lasers; lasers, injection-locked					
16. SECURITY CLASSIFICATION OF:			17. LIMITATION OF ABSTRACT: SAR	18. NUMBER OF PAGES 14	19a. NAME OF RESPONSIBLE PERSON (Monitor) Nicholas G. Usechak 19b. TELEPHONE NUMBER (Include Area Code) N/A
a. REPORT Unclassified	b. ABSTRACT Unclassified	c. THIS PAGE Unclassified			

# Dynamic behavior of an injection-locked quantum-dash Fabry-Perot laser at zero-detuning

M. Pochet<sup>1\*</sup>, N. A. Naderi<sup>1</sup>, N. Terry<sup>2</sup>, V. Kovanis<sup>2</sup>, L. F. Lester<sup>1</sup>

<sup>1</sup> Center for High Technology Materials, University of New Mexico, 1313 Goddard SE, Albuquerque, NM 87106, USA

<sup>2</sup> US Air Force Research Laboratory, 2241 Avionics Circle, WPAFB, OH 45433, USA

\*mpochet@unm.edu

**Abstract:** This work investigates the behavior of a zero-detuned optically-injected quantum-dash Fabry-Perot laser as the injected field ratio is increased from near-zero to levels resulting in stable locking. Using a normalized model describing optically-injected semiconductor lasers, variations in the slave laser's free-running characteristics are shown to have a strong impact on the coupled system's behavior. The theoretical model is verified experimentally using a high resolution spectrometer. It is found that the quantum-dash laser has the technological advantage of a low linewidth enhancement factor at low bias currents that suppresses undesirable Period-2 and chaotic behavior. Such observations suggest that optically-injected quantum-dash lasers can be used as an enabling component for tunable photonic oscillators.

©2009 Optical Society of America

**OCIS codes:** (140.5960) Semiconductor lasers; (140.3520) Lasers, injection-locked.

---

## References and links

1. T. Erneux, V. Kovanis, A. Gavrielides, and P. M. Alsing, "Mechanism for period-doubling bifurcation in a semiconductor laser subject to optical injection," *Phys. Rev. A* **53**(6), 4372 (1996).
2. L. F. Lester, N. Terry, A. Moscho, M. Fanto, N. Naderi, Y. Li, and V. Kovanis, "Giant Nonlinear Gain Coefficient of an InAs/AlGaInAs Quantum Dot Laser," *Proc. SPIE* **6889**, 68890M.1–68890M.8 (2008).
3. T. B. Simpson, J. M. Liu, A. Gavrielides, V. Kovanis, and P. M. Alsing, "Period-doubling cascades and chaos in a semiconductor laser with optical injection," *Phys. Rev. A* **51**(5), 4181–4185 (1995).
4. P. M. Alsing, V. Kovanis, A. Gavrielides, and T. Erneux, "Lang and Kobayashi phase equation," *Phys. Rev. A* **53**(6), 4429–4434 (1996).
5. S. K. Hwang, H. F. Chen, and C. Y. Lin, "All-optical frequency conversion using nonlinear dynamics of semiconductor lasers," *Opt. Lett.* **34**(6), 812 (2009).
6. F. Mogensen, H. Olesen, and G. Jacobsen, "Locking Conditions and Stability Properties for a Semiconductor Laser with External Light Injection," *IEEE J. Quantum Electron.* **QE-21**, 7 (1985).
7. J. M. Liu, *Applications of Nonlinear Dynamics* (Springer Berlin / Heidelberg, 2009), pages 341–354.
8. T. B. Simpson, and J. M. Liu, "Enhanced Modulation Bandwidth in Injection-Locked Semiconductor Lasers," *IEEE Photon. Technol. Lett.* **9**(10), 1322–1324 (1997).
9. D. Goulding, S. P. Hegarty, O. Rasskazov, S. Melnik, M. Hartnett, G. Greene, J. G. McInerney, D. Rachinskii, and G. Huyet, "Excitability in a Quantum Dot Semiconductor Laser with Optical Injection," *Phys. Rev. Lett.* **98**(15), 153903 (2007).
10. N. Naderi, M. Pochet, F. Grillot, N. Terry, V. Kovanis, and L. F. Lester, "Modeling the Injection-Locked Behavior of a Quantum Dash Semiconductor Laser," *IEEE J. Sel. Top. Quantum Electron.* **15**(3), 563–571 (2009).
11. F. Grillot, N. Naderi, M. Pochet, C.-Y. Lin, and L. F. Lester, "Variation of the feedback sensitivity in a 1.55 $\mu$ m InAs/InP quantum-dash Fabry-Perot semiconductor laser," *Appl. Phys. Lett.* **93**(19), 191108 (2008).
12. G. Liu, X. Jin, and S. L. Chuang, "Measurement of linewidth enhancement factor of semiconductor lasers using an injection-locking technique," *IEEE Photon. Technol. Lett.* **13**(5), 430–432 (2001).
13. A. Villafranca, G. Giuliani, S. Donati, and I. Garces, "Investigation on the linewidth enhancement factor of multiple longitudinal mode semiconductor lasers," *Proc. SPIE* **6997**, 699719.1–699719.8 (2008).

---

## 1. Introduction

This work theoretically describes and experimentally verifies the behavior of a zero-detuned quantum-dash (QDash) Fabry-Perot (FP) laser subjected to optical injection based on the

#112889 - \$15.00 USD Received 16 Jun 2009; revised 17 Sep 2009; accepted 6 Oct 2009; published 26 Oct 2009

(C) 2009 OSA

9 November 2009 / Vol. 17, No. 23 / OPTICS EXPRESS 20623

injected field ratio and the slave laser's free-running parameters. It is technologically significant that the low above-threshold linewidth enhancement factor ( $\alpha$ -factor) found in the QDash laser at bias levels close to threshold ( $<1.33\times$  threshold) inhibits Period-2 (P2) and chaotic operation [1–4]. The zero-detuned condition is also significant since it simplifies simulation and is easy to achieve experimentally. Only two behavioral states are observed at low bias conditions under zero-detuning as the injected field ratio is varied, Period 1 (P1) and stable locking, both of which can be used for novel applications [5–8]. The nonlinear dynamics of P1 operation has the potential for use in all optical frequency conversion and use as a building block for a tunable photonic oscillator for a whole host of RF photonic applications [5, 7]. The stable locking condition under strong injected power ratios is characterized by improved modulation characteristics to include bandwidth enhancement, reduced chirp, and reduced linewidth [6–8].

Using a normalized model representing optically-injected semiconductor lasers, the behavioral state (i.e. stable locking, Period-1, Period-2, or chaos) is theoretically evaluated as a function of the injected field ratio for varied slave laser bias conditions [1, 2, 7]. The normalized model used is advantageous compared with other approaches due to its fundamental parameter scaling approach that facilitates the comparison of one laser to another [9]. The P1 state, illustrated in Fig. 1(a), is characterized by the presence of relaxation oscillation sidebands [1–5]. Figure 1(b) shows the P2 state, also referred to as period doubling, which is similar to the P1 state but with additional side-bands associated with a periodic oscillator at roughly half the relaxation oscillation frequency. Stable locking is shown in Fig. 1(c) and is characterized by single mode operation with a significant degree of side mode suppression (defined here as  $> 30\text{dB}$ ), where the single locked-mode has a narrow linewidth, reduced chirp and noise compared to the slave laser's free running characteristics. The small side modes (side mode suppression  $> 40\text{ dB}$ ) in Fig. 1(c) are attributed to feedback in the experimental setup. The chaotic state, pictured in Fig. 1(d) is characterized by a large broadening of the coupled system's linewidth.

The  $\alpha$ -factor is shown to have a strong impact on the level of stability exhibited by the optically-injected QDash device at low injected field ratios [1]. An approach to approximate the injected field ratio needed to transition from P1 to stable locking (reverse-bifurcation point) is given. The importance of this value is that it indicates the injection condition above which stable locking is ensured and the benefits of stable injection-locking are realized [6–8].

The second part of this paper experimentally examines the validity of the model by employing a high resolution spectrometer to observe spectra of the optically injected QDash FP laser with zero-detuning between the master and slave; the master laser power is increased from extremely weak levels to levels corresponding to stable locking conditions. The experimental spectra are used to examine the validity of the numerical reverse-bifurcation point approximation. Although previous work has not shown a strong agreement between theoretical and experimental work examining the operational behavior of the QDash FP laser structure [2], the approach used here shows strong agreement as the relevant parameters driving the simulation were calculated using an approach that accounts for the large inverse spontaneous carrier lifetime of the device and implicitly incorporates non-linear gain through measured data. The data set is unique in nature due to the high resolution of the spectrometer used (1 MHz), which allows extreme detail of the coupled system's behavior to be observed. Goulding et al. [9] indicate a similar result for an InAs quantum dot laser, where only stable

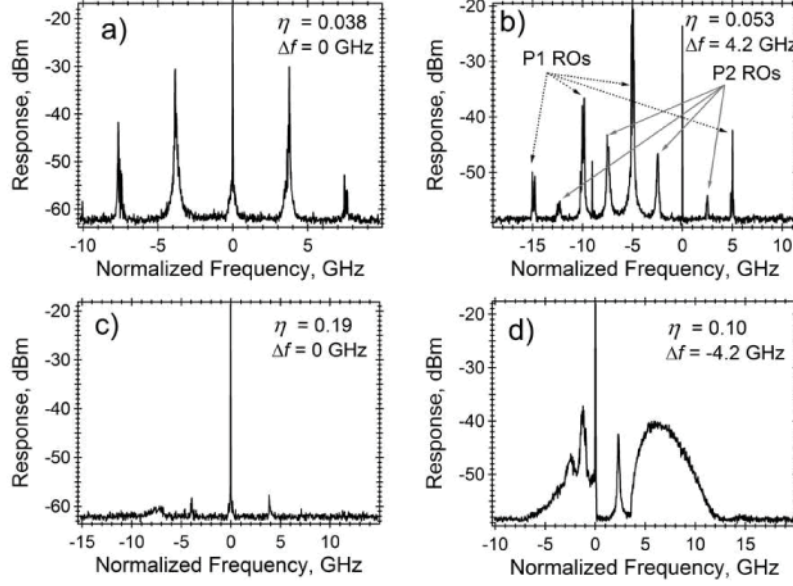


Fig. 1. Operational states of an optically injected system; experimentally collected using the high resolution spectrometer: (a) the Period-1 state showing strong relaxation oscillations; (b) the Period-2 state showing both the Period-1 & Period-2 relaxation oscillations; (c) the locked state showing single mode operation; and (d) the chaotic state. For all cases the slave laser bias was 60 mA.

locking is reported under zero-detuning conditions. The results reported here are in general agreement with those presented in [9] for low QDash laser bias conditions, highlighting the benefits of low  $\alpha$ -factor laser devices. The data set presented here is unique due to the focus on the zero-detuning condition, where a small step size and extremely low values of injected power were used experimentally, as the Period-1, Period-2, and chaotic behaviors are typically only observed over a small window of low injected field ratios [1].

## 2. Theory

The normalized rate equations used to analyze the optically injected system are given in Eqs. (1) - (3) and describe the amplitude of the electric field  $E$ , the phase difference between the master and slave electric field  $\psi$ , and the carrier density above threshold  $N$  [1].

$$\frac{dE}{d\tau} = NE + \eta \cos(\psi) \quad (1)$$

$$\frac{d\psi}{d\tau} = \Delta - \alpha N - \eta E^{-1} \sin(\psi) \quad (2)$$

$$T \frac{dN}{d\tau} = P - N - P(1 + 2N)E^2 \quad (3)$$

where the time,  $\tau$ , is normalized to the photon lifetime ( $\tau = t/\tau_p$ ).  $T$  is the ratio of the cavity decay rate,  $\gamma_C$ , (where  $\gamma_C = 1/\tau_p$ ) to the inverse carrier lifetime,  $\gamma_S$ , such that  $T = (\gamma_C / \gamma_S)$ . Both  $\gamma_S$  &  $\gamma_C$  are independent of slave laser output power, making  $T$  a constant for a given slave laser [1]. The injected field ratio within the slave laser cavity is given by  $\eta$ , and  $\alpha$  is the linewidth enhancement factor.  $P$  is proportional to the pumping current above threshold, and is calculated using  $P = (1/2)(\gamma_N/\gamma_S) \propto (J - J_{th})/J_{th}$  [1, 4], where  $J$  is the injected current density and  $J_{th}$  is the threshold current density.  $\gamma_N$  is the differential carrier relaxation rate normalized

to the photon lifetime, and is equal to  $\tau_p G_M(J - J_{th})/qd$ . In this expression  $G_M$  is the differential gain with respect to carrier density, and  $d$  is the active region thickness [4].  $\Delta$  is the frequency offset between the master and slave laser fields, and is held constant at zero both analytically and experimentally in this work. Non-linear gain is not included in this model above for simplicity; however, it is implicitly incorporated in the free-running relaxation oscillation frequency,  $\omega_R$ , and the damping rate,  $\gamma_R$ , via direct experimental measurement of these parameters [10]. The free-running relaxation rate, normalized to the photon lifetime  $\tau_p$ , is given by  $\omega_r^2 = 2P/T$ , and the normalized free-running damping rate is given by  $\gamma_R = (1+2P)/T = \gamma_S + \gamma_N + \gamma_P$  [4]. In the latter case,  $\gamma_P$  is the non-linear carrier relaxation term with respect to the photon density in the cavity. Thus, knowing the free-running damping rate, relaxation oscillation frequency, photon lifetime, and spontaneous carrier lifetime allows the  $P$ - and  $T$ -parameters to be calculated for a given slave laser bias current. These  $P$ - and  $T$ -values combined with the  $\alpha$ -factor characterized as a function of bias current allows the optically-injected laser to be accurately simulated using the normalized model. It is by calculating the  $P$ -value based on the free-running relaxation and damping rate that non-linear gain is implicitly incorporated.

Using the normalized model, the coupled differential equations describing the IL system can be solved in the time domain, and qualitative changes can be observed in the electric field solution. For this work, the electric field solution is analyzed as the injected field ratio,  $\eta$ , is varied. The qualitative change, i.e. bifurcations, to the electric field's time response as a solution to Eqs. (1) - (3) for zero-detuning conditions is plotted as a function of the injected field ratio. Bifurcation diagrams for various slave laser bias conditions are given in Fig. 2, where the y-axis represents  $E/E_s$  with  $E_s$  the free-running electric field amplitude and  $E$  is the amplitude of the electric field solution. The  $P$ - &  $T$ -parameter and  $\alpha$ -factor values were representative of varied slave laser bias conditions for the QDash FP slave laser under test, as QDash devices of this structure have been found to possess an  $\alpha$ -factor that varies greatly as a function of the bias current [11]. Specifically, QDash devices of this structure have been demonstrated to have an  $\alpha$ -factor that increases from  $\sim 1$  to  $\sim 14$  as the bias current is increased from threshold to approximately twice the threshold value. This value was measured using the injection-locking technique which is based on the asymmetry of the stable locking range of detuning on both the positive and negative side of the locked mode [12]. The photon lifetime,  $\tau_p$ , for the QDash FP device was measured to be 3 ps, based on the cavity length, mirror reflectivity, and measured waveguide internal loss. The inverse spontaneous carrier lifetime,  $\gamma_S$ , was 6 GHz. The bifurcation diagrams show that as the  $\alpha$ -factor and  $P$ -parameter increase with bias current, a larger injected field ratio is necessary to achieve stable locking; stable locking is characterized in the diagrams by a single extrema value observed in the electric field solution. Additionally, the numerical simulations in Fig. 2 show that as the  $\alpha$ -factor is increased from 2.2 to 6.0, more chaotic states are observed in the solution at lower injected field ratios. Figure 2 also shows that the 'bubble' indicating operational states other than stable locking increases in size as the  $\alpha$ -factor and  $T$ -parameter increase with bias current. The QDash laser is unique in allowing examination of dynamics over a large range of  $\alpha$ -factor within a single device.

Quantitatively [1], estimates the bifurcation and reverse bifurcation points marking the transition from stable-to-P1 ( $\eta_1$ ) and P1-to-stable ( $\eta_2$ ) using the following expressions:

$$\eta_1 = (1+2P)(1+\alpha^2)^{1/2}T^{-1}(\alpha^2-1)^{-1} = \frac{(1+\alpha^2)^{1/2}}{\alpha^2-1}\gamma_R \approx \frac{1}{\alpha}\gamma_R \quad (4)$$

$$\eta_2 = [(\alpha^2-1)2P]^{1/2}T^{-1/2} = (\alpha^2-1)^{1/2}\omega_r \approx \alpha\omega_r \quad (5)$$

where both  $\omega_r$  and  $\gamma_R$  are normalized to the photon lifetime. Equations (4) and (5) show that  $\eta_1$  and  $\eta_2$  are strongly dependant on the slave laser  $\alpha$ -factor. The agreement between theoretical evaluations of the P1-to-stable point using Eq. (5) and the bifurcation diagrams in Fig. 2 is

shown in section 3.2. Equation (5) is significant in that once a slave laser's free-running relaxation

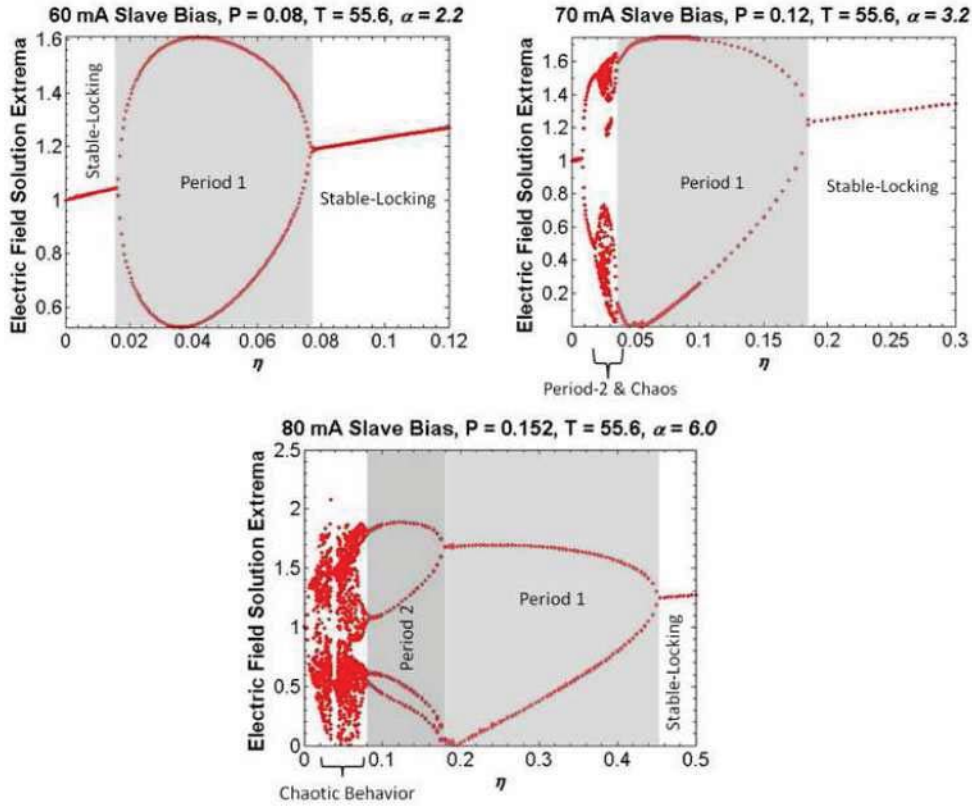


Fig. 2. Bifurcation diagrams showing theoretical solutions to Eqs. (1) - (3) for zero-detuning conditions. The three cases correspond to respective  $P$ ,  $T$ , and  $\alpha$ -factor values for 60mA, 70mA, and 80mA slave bias conditions and illustrate the dynamic nature of the QDash slave laser's operational behavior based on bias current.  $T$  is the same for all 3 cases, 55.6.

rate and  $\alpha$ -factor have been characterized based on bias current, the minimum injected field ratio necessary to ensure stable locking at zero-detuning can be approximated; this is important in system designs that require stable locking conditions to be met.

### 3. Experimental description and results

#### 3.1 Experimental description

The injection locking experimental setup is depicted in Fig. 3. The master laser was a New Focus 6200 external cavity tunable diode laser with a wavelength range from 1.4 – 1.6  $\mu\text{m}$ . The output of the master laser was fiber-pigtailed into a polarization maintaining (PM) single-mode fiber that was coupled into the second arm of a 3-port PM circulator. An erbium doped fiber amplifier (EDFA) and optical attenuator were placed between the master laser and the input to port 2 in order to vary the injected master laser power. A Yokogawa AQ6319 optical spectrum analyzer (OSA), with a resolution of 10 pm (1.25 GHz), was connected to port 3 of the circulator and used to monitor the spectra of the IL system. For a portion of the data collection, an Agilent high resolution spectrometer with a resolution of 1 MHz was used in place of the OSA. Zero wavelength detuning conditions were maintained between the master and slave, and the injected master laser power was varied in order to observe the optically injected system transition between behavioral states. The slave laser was a multi-mode QDash FP device grown on an  $\text{n}^+\text{-InP}$  substrate. A full description of the device can be found in [2].

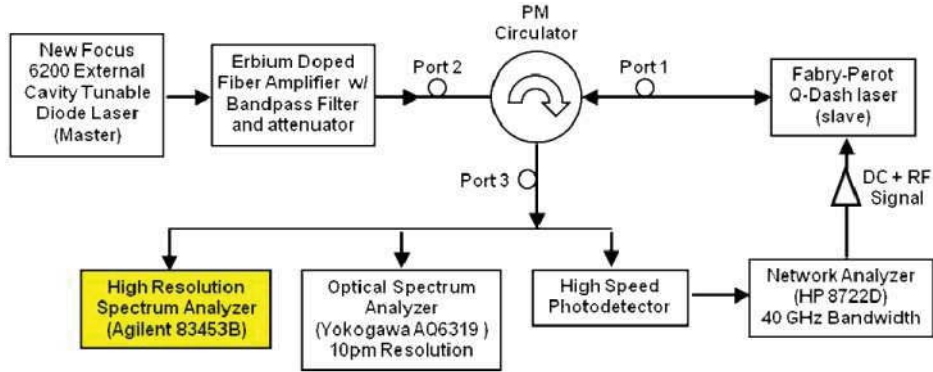


Fig. 3. Injection-locking experimental setup.

### 3.2 Experimental results

Experimental spectra associated with the 60mA bias case ( $\alpha$ -factor = 2.2) are given in Fig. 4, which correspond to the simulated case in Fig. 2(a). The spectra shown in Fig. 4, collected with the Agilent high resolution spectrometer, correspond to injected field ratio values at the experimental bifurcation (stable-P1 transition) and reverse-bifurcation (P1-stable transition) points, as well as values within the P1 ‘bubble’, and within the upper stable locking regions. The spectra confirm the agreement between the simulated and numerical results.

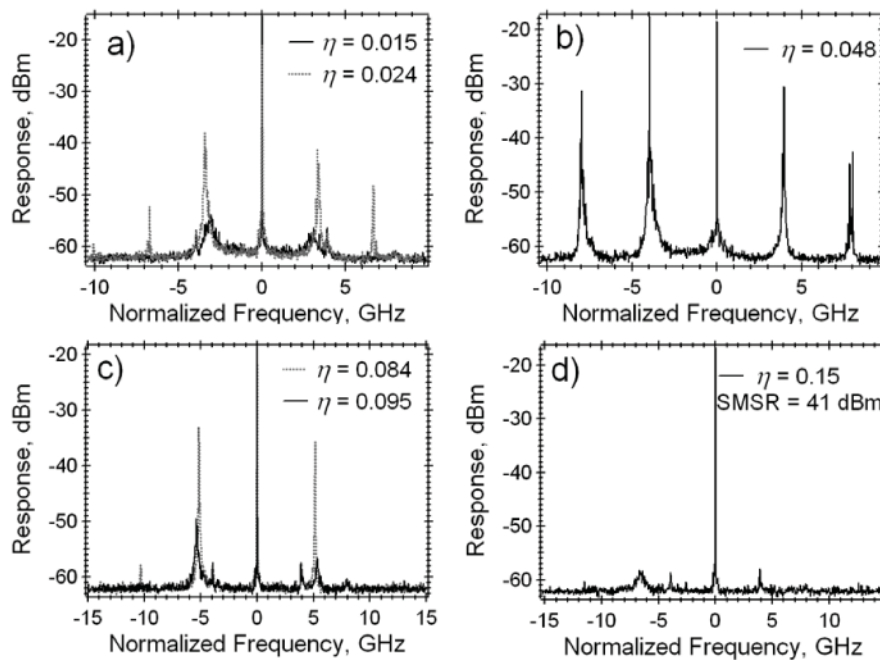


Fig. 4. Experimental spectra associated with the 60mA slave bias case shown theoretically in Fig. 3(a). The injected field ratio values for the individual plots correspond to the experimental bifurcation and reverse bifurcation points, as well as Period-1 and stable conditions. (a) Lower stable locking regime; (b) bifurcation point transition from stable to Period-1; (c) Period-1 regime; (d) reverse bifurcation from Period-1 to stable; and (e) upper stable locking regime. Normalized from 191.914 THz.

Table 1 shows the injected field ratio observed at the P1-to-stable boundary (reverse-bifurcation point) found using various methods: calculated using Eq. (5); extracted from the numerical bifurcation diagram; and the experimentally observed value. For the 65 mA, 70

mA, 75 mA, and 80 mA slave bias cases, the OSA (Yokogawa AQ6319) with 10 pm (1.25 GHz) resolution was used to monitor the optical spectrum under injection. The Agilent HRS was used for only the 60 mA slave bias case. Although the Yokogawa OSA did not have the resolution of the Agilent HRS used to produce the spectrum shown in Figs. 1 & 4, it did allow for the relaxation oscillation peaks to be observed with ample resolution and the SMSR to be measured. The drawback of the Yokogawa OSA is that zero-detuning conditions can only be achieved within the 10 pm (1.25 GHz) resolution. The experimental injected field ratio  $\eta_{exp}$  was calculated using Eq. (6), where  $P_{master}$  is the external master power at the slave laser facet,  $K$  is the fiber coupling efficiency, and  $P_{slave}$  is the external slave power.

$$\eta_{exp} = \frac{(1-R)}{\sqrt{R}} \sqrt{\frac{P_{master} K}{P_{slave}}} \quad (6)$$

The  $(1-R)/(R)^{1/2}$  term relates the internal to external field ratios [11]. The coupling efficiency ranged from 10 to 50%. Experimentally, the injection ratio at the bifurcation point ( $\eta_1$ ) transitioning from stable locking to P1 is difficult to measure accurately as it occurs at extremely low injected master laser powers that can be hard to control. Thus, the relation between the theoretical and experimental values was only compared qualitatively for this transition point, which was observed to show corresponding trends. The injected field ratio at the reverse bifurcation point ( $\eta_2$ ) computed using Eq. (5) and the corresponding value gathered experimentally shown in Table 1 are in good agreement for the 60 mA slave bias case, as the spectra under this bias were collected using the HRS and the detuning was controlled to greater accuracy. The 65-80 mA experimental data shown the same monotonically increasing  $\eta_2$  with the  $\alpha$ -factor as the theory, but the quantitative agreement is not as strong. A portion of this deviation is attributed to the use of the OSA and as strong an ability to control the detuning conditions only to within 10 pm, which theoretically is shown to introduce an error of up to 5%. This deviation is due to the fact that when the master and slave laser are detuned from one another, a higher injected field ratio is needed to achieve stable locking. It is also noted that the accuracy of the model is highly dependant on the accuracy of the measured  $\alpha$ -factor, and thus any error in the measured above-threshold  $\alpha$ -factor will propagate into the model. It has been reported that measurements of the  $\alpha$ -factor can vary by +/- 40%, and also vary for different longitudinal modes for a FP laser [13]. Table 1 shows the stable locking threshold ( $\eta_2$ ) is strongly dependant on the  $\alpha$ -factor.

**Table 1. Numerically Calculated and Experimentally Observed Reverse Bifurcation Injection Field Ratio ( $\eta_2$ ) Values**

$I_{slave}$ (mA)	$\alpha$	$\omega_r$ (GHz)	$\eta_{exp}$	$\eta_2$ (calculated using Eq. (5))	$\eta_2$ (from numerical bifurcation diagram)
60	2.2	17.9	0.10	0.105	0.084
65	2.5	19.7	0.54	0.136	0.12
70	3.2	21.6	0.55	0.197	0.19
75	3.9	23.1	0.67	0.261	0.26
80	6	24.6	0.71	0.437	0.47

#### 4. Conclusions

The analysis presented in this manuscript shows that the single-mode rate equations faithfully predict the dynamical response exhibited by a zero-detuned optically-injected semiconductor system for varied injected field ratios. At zero-detuning and at bias currents close to threshold, the response is observed to transition from a locked state at extremely low injection levels to a P1 state, returning to stable locking under strong injection locking conditions; this is significant as no P2 or chaotic states (coherence collapse) are observed. Such measurements

in various semiconductor lasers, including vertical cavity lasers and DFBs, have shown a period-doubling route into chaos. Numerical simulations show that this novel behavior is due to the QDash devices' characteristically low  $\alpha$ -factor close to the threshold condition and its high inverse carrier lifetime. At slave laser bias conditions well above threshold which result in increased  $\alpha$ -factor values, the characteristic behavior of the optically injected laser changes and regions of coherence collapse and P2 behaviors are predicted at low injected field ratios. Due to the large variation of the  $\alpha$ -factor with bias current, it was possible to observe the change in the P1 to stable locking reverse bifurcation point within a single QDash slave laser as function of bias current. Additionally, the emergence of P2 behavior at bias currents well above threshold was observed at low injected field ratios and are primarily attributed to the enhancement of the  $\alpha$ -factor with increased bias current. The optical power spectra recorded was shown to be in qualitative agreement with the numerical simulation of the single mode rate equations. Such simple behavior, frequency tunability, and absence of coherence collapse at low bias conditions on the online dynamics coupled with wavelength emission at 1550 nm suggest that an optically-injected QDash @1550nm may be an appropriate building block for a tunable photonic oscillator for a whole host of RF photonic applications.

### **Acknowledgment**

This work was supported by the U.S. Air Force Research Laboratory under Grant FA8750-06-1-0085. V. Kovanis and N. Terry were funded by AFOSR LRIR 09RY04COR. The views expressed in this article are those of the author & do not reflect the official policy or position of the United States Air Force, Department of Defense, or the U.S. Government.